Firstorder nonadiabatic coupling matrix elements from multiconfigurational self consistentfield response theory

Keld Lars Bak, Poul Jo/rgensen, Hans Jo/rgen Aa. Jensen, Jeppe Olsen, and Trygve Helgaker

Citation: The Journal of Chemical Physics **97**, 7573 (1992); doi: 10.1063/1.463477
View online: http://dx.doi.org/10.1063/1.463477
View Table of Contents: http://scitation.aip.org/content/aip/journal/jcp/97/10?ver=pdfcov
Published by the AIP Publishing

First-order nonadiabatic coupling matrix elements from multiconfigurational self-consistent-field response theory

Keld Lars Bak and Poul Jørgensen
Department of Chemistry, Aarhus University, DK-8000 Aarhus C, Denmark

Hans Jørgen Aa. Jensen
Department of Chemistry, Odense University, DK-5230 Odense M, Denmark

Jeppe Olsen
Theoretical Chemistry, Chemistry Center, University of Lund, Box 124, S-22100 Lund, Sweden

Trygve Helgaker
Department of Chemistry, University of Oslo, Blindern, N-0315 Oslo 3, Norway

(Received 4 June 1992; accepted 3 August 1992)

A new scheme for obtaining first-order nonadiabatic coupling matrix elements (FO-NACME) for multiconfigurational self-consistent-field (MCSCF) wave functions is presented. The FO-NACME are evaluated from residues of linear response functions. The residues involve the geometrical response of a reference MCSCF wave function and the excitation vectors of response theory. Advantages of the method are that the reference state is fully optimized and that the excited states, represented by the excitation vectors, are strictly orthogonal to each other and to the reference state. In a single calculation the FO-NACME between the reference state and several excited states may be obtained simultaneously. The method is most well suited to describe situations where the dominant configurations for the two states differ mainly by a single electron replacement. When the dominant configurations differ by two electrons many correlating orbitals are required in the MCSCF reference state calculation to accurately describe the FO-NACME. FO-NACME between various states of H_2, MgH_2, and BH are presented. These calculations show that the method is capable of giving quantitatively correct results that converge to the full configuration interaction limit. Comparisons are made with state-averaged MCSCF results for MgH_2 and finite-difference configuration interaction by perturbation with multiconfigurational zeroth-order wave function reflected by interactive process (CIPSI) results for BH.

I. INTRODUCTION

The adiabatic or Born–Oppenheimer approximation[1] has, since its formulation in 1927, proven very successful in describing many chemical processes. However, the interpretation of many observations requires corrections to the adiabatic approximation. Such observations or phenomena are usually termed nonadiabatic. Examples of nonadiabatic phenomena found in molecular spectroscopy are Λ doubling and line shifts, whose size can be small[2] or large[3] depending on the strength of the nonadiabatic couplings. Forbidden transitions and predissociations also occur as results of nonadiabatic couplings and in reaction dynamic studies the nonadiabatic couplings are responsible for electronic transitions such as exchange excitations and charge-transfer reactions.[4]

Not surprisingly, a great deal of effort has been devoted to the development of theories for treating nonadiabatic phenomena and to qualitative and quantitative calculations of such phenomena. Approaching nonadiabatic problems using adiabatic electronic wave functions involves the evaluation of nonadiabatic coupling matrix elements (NACME). A variety of approaches have been used for this purpose. The Landau–Zener approximation constitutes a very simple method where the coupling between electronic states are considered.[5] Finite difference schemes for NACME have been presented both for configuration interaction (CI) and multiconfigurational self-consistent-field (MCSCF) type wave functions.[6,7] The finite difference scheme is simple but suffers from the difficulties related to numerical accuracy and computational efficiency.

The most accurate nonadiabatic *ab initio* calculations have been carried out on H_2 by Wolniewicz and Dressler.[8] The electronic wave functions used in their work are generalized James–Coolidge type functions, which depend explicitly on the interelectronic distance. The NACME for these wave functions are calculated analytically. For wave functions used for more general systems, Lengsfield, Saxe, and Yarkony have shown in a series of papers that the concept of state-averaged (SA) orbitals for MCSCF and multireference configuration interaction (MRCI) wave functions can be utilized to enable the analytic calculation of NACME with the same concepts as for molecular gradient calculations.[9]

The aim of this work is to present an alternative scheme for obtaining first-order NACME (FO-NACME) for MCSCF wave functions. The scheme is based on time-dependent response theory[10] and it uses many of the techniques developed for the analytical calculation of MCSCF molecular Hessians.[11] The NACME are evaluated from

 0021-9606/92/227573-12$006.00

residues of linear response functions for a reference MCSCF state. Advantages of the method are that the reference state is fully optimized and that the excited states, which are not explicitly calculated, are strictly orthogonal to each other and to the reference state. In a single calculation the FO-NACME between the reference state and a range of other states of the same or different symmetry as the reference state are obtained. The FO-NACME between two excited states may be obtained as residues of quadratic response functions. These elements can also be determined in calculations where one of those states are chosen as the reference state.

The method has been implemented and test calculations performed. In this work we present FO-NACME between various states of H_2, MgH_2, and BH. The H_2 calculations demonstrate that the method is capable of giving quantitatively correct results. The MgH_2 calculations enable a comparison to previous SA-MCSCF calculations on this system, and the BH calculations allow us to investigate in more detail the choice of MCSCF reference state and also give some interesting new nonadiabatic coupling functions.

For H_2 NACME between the lowest (B) and the next two (B' and $B''\overline{B}$) $^1\Sigma_u^+$ states are calculated. Our FO-NACME between the B and B' states agree with the essentially exact results of Wolniewicz and Dressler.[8a] We expect the calculated FO-NACME involving the B and the $B''\overline{B}$ states to be of the same quality as those between the B and B' states.

Lengsfield, Saxe, and Yarkony have previously presented FO-NACME for MgH_2 calculated by the SA-MCSCF method.[9a] We have used the same basis set and active space and the resulting NACME are very similar.

The calculations on BH concern the three lowest lying $^1\Sigma^+$ states X,B, and C. FO-NACME are calculated between the X and B states and between the B and C states. Using a common basis set we have extended the complete active state (CAS) and compared with full configuration interaction (FCI). The size of the CAS needed to obtain a given accuracy varies with the internuclear distance. The coupling function between the B and C states is compared with the recent calculations by Cimiraglia.[12] General agreement is obtained, but some differences are also observed.

Section II contains the theoretical derivations which show how FO-NACME can be evaluated from residues of the first-order response function for a given electronic state. The test calculations on H_2, MgH_2, and BH are presented in Sec. III. A short summary of the work is found in Sec. IV.

II. THEORY

In this section we use the language of second quantization and response function theory[10] to derive expressions for the calculation of the FO-NACME,

$$g_{n0}(\mathbf{x},b)=\langle n(\mathbf{x})|\frac{\partial}{\partial b}|0(\mathbf{x})\rangle. \tag{1}$$

$|0(\mathbf{x})\rangle$ and $|n(\mathbf{x})\rangle$ are adiabatic time-independent electronic wave functions that parametrically depend on the set of nuclear coordinates $\mathbf{x}$. The wave function $|0(\mathbf{x})\rangle$ is referred to as the reference state and the symbol b denotes an arbitrary nuclear coordinate.

We assume the reference state is a MCSCF wave function and specify in Sec. II A how this wave function is connected from one nuclear geometry to another, making it a function of the nuclear coordinates. We use finite basis sets clamped to the nuclei and first describe how a general differentiation of $|0(\mathbf{x})\rangle$ with respect to a nuclear coordinate is carried out. It is shown how this differentiation may be carried out using an effective operator that depends upon the wave function on which it acts. It is remarkable that this differentiation involves an explicit differentiation of the creation and annihilation operators. In contrast to energy derivative calculations, the dependence of the creation and annihilation operators on geometry cannot be neglected in calculations of NACME.

Response function theory has previously been shown to enable the calculation of transition matrix elements for time-independent operators.[10] In Sec. II B we use response function theory and the effective differentiation operator to derive expressions for FO-NACME that involve the reference state. The FO-NACME can, in this way, be evaluated following the same scheme as for transition moments.

A. Differentiation of the MCSCF reference state with respect to a nuclear coordinate

At a reference geometry $\mathbf{x}_0$ we assume that the reference state is an optimized MCSCF wave function expanded in a set of N configuration state functions (CSF),

$$|0(\mathbf{x}_0)\rangle=\sum_g C_{g0}(\mathbf{x}_0)|\phi_g(\mathbf{x}_0)\rangle, \tag{2}$$

where both the expansion coefficients $C_{g0}(\mathbf{x}_0)$ and the CSF $|\phi_g(\mathbf{x}_0)\rangle$ depend parametrically on the nuclear geometry. The CSF themselves are linear combinations of Slater determinants,

$$|\phi_g^S(\mathbf{x}_0)\rangle=\prod_{i\in Sg} a_i^\dagger(\mathbf{x}_0)|\text{vac}\rangle, \tag{3}$$

where $\Pi_{i\in Sg}a_i^\dagger(\mathbf{x}_0)$ denote an ordered product of creation operators. The creation operator $a_i^\dagger(\mathbf{x}_0)$ creates an electron in the MCSCF spin orbital $\varphi_i(\mathbf{x}_0)$, which is spanned in a finite space defined by the set of atomic orbitals (AO) $\{\chi_\mu(\mathbf{x}_0)\}$

$$\varphi_i(\mathbf{x}_0)=\sum_\mu K_{\mu i}(\mathbf{x}_0)\chi_\mu(\mathbf{x}_0). \tag{4}$$

The set of MCSCF orbital coefficients $\{K_{\mu i}(\mathbf{x}_0)\}$ and the CI coefficients $\{C_{g0}(\mathbf{x}_0)\}$ are found from the generalized Brillouin theorem

$$\begin{aligned}&\langle 0(\mathbf{x}_0)|[q^+(\mathbf{x}_0),H_0(\mathbf{x}_0)]|0(\mathbf{x}_0)\rangle=0,\\&\langle 0(\mathbf{x}_0)|[R^+(\mathbf{x}_0),H_0(\mathbf{x}_0)]|0(\mathbf{x}_0)\rangle=0.\end{aligned} \tag{5}$$

The operators $q^+(\mathbf{x}_0)$ and $R^+(\mathbf{x}_0)$ of Eq. (5) belong to the manifold

$$[T(\mathbf{x}_0)]=[q^+(\mathbf{x}_0),R^+(\mathbf{x}_0),q(\mathbf{x}_0),R(\mathbf{x}_0)] \tag{6}$$

and are defined by

$$q_{ij}^\dagger(\mathbf{x}_0)\equiv a_i^\dagger(\mathbf{x}_0)a_j(\mathbf{x}_0), \quad i>j \tag{7a}$$

and

$$R_r^\dagger(\mathbf{x}_0)\equiv|r(\mathbf{x}_0)\rangle\langle 0(\mathbf{x}_0)|, \quad |r(\mathbf{x}_0)\rangle\neq|0(\mathbf{x}_0)\rangle. \tag{7b}$$

In Eq. (6) $R_r(\mathbf{x}_0)$ and $q_{ij}(\mathbf{x}_0)$ are the adjoints of $R_r^\dagger(\mathbf{x}_0)$ and $q_{ij}^\dagger(\mathbf{x}_0)$. In the space defined by the CSF that span $|0(\mathbf{x}_0)\rangle$, the set of states $\{|r(\mathbf{x}_0)\rangle\}$ spans the orthogonal complement to $|0(\mathbf{x}_0)\rangle$

$$|r(\mathbf{x}_0)\rangle=\sum_g^N C_{gr}(\mathbf{x}_0)|\phi_g(\mathbf{x}_0)\rangle. \tag{8}$$

Due to the geometry dependence of the basis, the MCSCF state in Eq. (2) is defined at the reference geometry only. To extend its definition to other geometries we introduce a set of so-called unmodified molecular orbitals (UMO)

$$\psi_i(\mathbf{x})=\sum_\mu K_{\mu i}(\mathbf{x}_0)\chi_\mu(\mathbf{x}). \tag{9}$$

The expansion coefficients of the UMO are geometry independent and equal to the MCSCF molecular-orbital expansion coefficients at $\mathbf{x}_0$. Except for $\mathbf{x}=\mathbf{x}_0$, these UMO *cannot* be expected to be orthonormal:

$$S_{ij}(\mathbf{x})\equiv\langle\psi_i(\mathbf{x})|\psi_j(\mathbf{x})\rangle=\sum_{\mu\nu}K_{\mu i}(\mathbf{x}_0)K_{\nu j}(\mathbf{x}_0)\mathbf{S}_{\mu\nu}^{\mathrm{AO}}(\mathbf{x}). \tag{10}$$

The $\mathbf{S}^{\mathrm{AO}}(\mathbf{x})$ matrix on the right-hand side of Eq. (10) is the AO overlap matrix at the geometry $\mathbf{x}$. Provided the overlap matrix for the UMO $\mathbf{S}(\mathbf{x})$ in Eq. (10) is nonsingular, we can define a set of orthonormal molecular orbitals (OMO) at an arbitrary geometry $\mathbf{x}$ as linear combinations of UMO

$$\varphi_i(\mathbf{x})\equiv\sum_j T_{ji}(\mathbf{x})\psi_j(\mathbf{x}). \tag{11}$$

We choose an orbital connection where the matrix $\mathbf{T}(\mathbf{x})$ equals $\mathbf{S}^{-1/2}(\mathbf{x})$. The matrix $\mathbf{T}(\mathbf{x})$ and its matrix elements in Eq. (11) should *not* be confused with the operator manifold $[T(\mathbf{x}_0)]$ of Eq. (6).

The CSF at any geometry $\mathbf{x}$ may now be expressed in terms of creation operators $\{a_i^\dagger(\mathbf{x})\}$ associated with the OMO. We next define an unoptimized MCSCF expansion at geometry $\mathbf{x}$,

$$|0(\mathbf{x})\rangle=\sum_g C_{g0}(\mathbf{x}_0)|\phi_g(\mathbf{x})\rangle, \tag{12}$$

with the expansion coefficients $C_{g0}(\mathbf{x}_0)$ taken to be geometry independent and equal to the expansion coefficients at $\mathbf{x}_0$.

The relaxed or optimized reference state at $\mathbf{x}$ is created by a unitary transformation of $|0(\mathbf{x})\rangle$ in the orbital and the configuration space:

$$|\tilde{0}(\mathbf{x})\rangle=\exp\Big(\sum_{i>j}\kappa_{ij}(\mathbf{x})q_{ij}^-(\mathbf{x})\Big)\times\exp\Big(\sum_{r\neq 0}P_r(\mathbf{x})R_r^-(\mathbf{x})\Big)|0(\mathbf{x})\rangle. \tag{13}$$

The two sets of variationally optimized coefficients $\kappa_{ij}(\mathbf{x})$ and $P_r(\mathbf{x})$ determine the MCSCF state at geometry $\mathbf{x}$. Since $|0(\mathbf{x})\rangle$ corresponds to an optimized state at $\mathbf{x}_0$, the variables $\kappa_{ij}(\mathbf{x})$ and $P_r(\mathbf{x})$ become zero for $\mathbf{x}=\mathbf{x}_0$. The operators in Eq. (13) are defined as

$$q_{ij}^-(\mathbf{x})\equiv q_{ij}^\dagger(\mathbf{x})-q_{ij}(\mathbf{x}), \tag{14a}$$

$$R_r^-(\mathbf{x})\equiv R_r^\dagger(\mathbf{x})-R_r(\mathbf{x}). \tag{14b}$$

Taking the derivative of the variationally optimized reference wave function with respect to the nuclear coordinate b at $\mathbf{x}_0$ we obtain

$$\begin{aligned}\frac{\partial}{\partial b}|\tilde{0}(\mathbf{x})\rangle|_{\mathbf{x}=\mathbf{x}_0}&=\sum_{i>j}\kappa_{ij}^{(b)}(\mathbf{x}_0)q_{ij}^-(\mathbf{x}_0)|0(\mathbf{x}_0)\rangle+\sum_{r\neq 0}P_r^{(b)}(\mathbf{x}_0)\\&\times R_r^-(\mathbf{x}_0)|0(\mathbf{x}_0)\rangle+\sum_g C_{g0}(\mathbf{x}_0)\\&\times\sum_i a_1^\dagger(\mathbf{x}_0)\cdots\cdots\frac{\partial a_i^\dagger(\mathbf{x})}{\partial b}\Big|_{\mathbf{x}=\mathbf{x}_0}\cdots|\mathrm{vac}\rangle,\end{aligned} \tag{15}$$

where

$$\kappa_{ij}^{(b)}(\mathbf{x})\equiv\frac{\partial\kappa_{ij}(\mathbf{x})}{\partial b}, \tag{16a}$$

$$P_r^{(b)}(\mathbf{x})\equiv\frac{\partial P_r(\mathbf{x})}{\partial b}. \tag{16b}$$

It should be emphasized that although the creation operators refer to orthonormal orbitals, their differentiation in Eq. (15) cannot be neglected. This is in contrast to calculations of adiabatic properties such as molecular gradients and Hessians where matrix elements are differentiated with respect to nuclear coordinates. In such calculations the total effect of differentiations involving the creation and annihilation operators reduces to a differentiation of coupling matrices. For an orthonormal basis these are constant and the differentiation gives zero. We can therefore ignore the geometry dependence of creation and annihilation operators when adiabatic properties like molecular gradients and Hessians are calculated in orthonormal bases.[11,13] The same arguments do not hold for calculations of NACME.

The derivative of a creation operator $\partial a_i^\dagger(\mathbf{x})/\partial b$ is a new operator that creates an electron in the orbital $\partial\varphi_i(\mathbf{x})/\partial b$. This orbital is divided into two parts, one of which may be expanded in the set of OMO at $\mathbf{x}$ and a second part which is orthogonal to the space spanned by the OMO at $\mathbf{x}$. Defining $\varphi_{\perp i}(\mathbf{x})$ as the part of $\partial\varphi_i(\mathbf{x})/\partial b$ that is orthogonal to the space spanned by the OMO at $\mathbf{x}$, we have

$$\frac{\partial\varphi_i(\mathbf{x})}{\partial b}=\sum_j D_{ji}^{(b)}(\mathbf{x})\varphi_j(\mathbf{x})+\varphi_{\perp i}(\mathbf{x}), \tag{17}$$

where

$$D_{ji}^{(b)}(\mathbf{x})\equiv\left\langle\varphi_j(\mathbf{x})\left|\frac{\partial\varphi_i(\mathbf{x})}{\partial b}\right.\right\rangle. \tag{18}$$

Inserting Eq. (11) into Eq. (18), and using the fact that the UMO equals the MCSCF orbitals for $\mathbf{x}=\mathbf{x}_0$, we obtain

$$D_{ji}^{(b)}(\mathbf{x}_0)=\left\langle\varphi_j(\mathbf{x}_0)\left|\frac{\partial\psi_i(\mathbf{x})}{\partial b}\right|_{\mathbf{x}=\mathbf{x}_0}\right\rangle+\left.\frac{\partial T_{ji}(\mathbf{x})}{\partial b}\right|_{\mathbf{x}=\mathbf{x}_0}. \tag{19}$$

Since $\mathbf{S}(\mathbf{x})$ is the identity matrix at $\mathbf{x}=\mathbf{x}_0$, the derivative of an element of $\mathbf{S}^{-1/2}(\mathbf{x})$ with respect to a nuclear coordinate b at $\mathbf{x}=\mathbf{x}_0$ is

$$\left.\frac{\partial T_{ji}(\mathbf{x})}{\partial b}\right|_{\mathbf{x}=\mathbf{x}_0}=-\frac{1}{2}\frac{\partial}{\partial b}\langle\psi_j(\mathbf{x})\,|\,\psi_i(\mathbf{x})\rangle|_{\mathbf{x}=\mathbf{x}_0}. \tag{20}$$

For real OMO Eq. (19) gives

$$D_{ji}^{(b)}(\mathbf{x}_0)=\frac{1}{2}\Bigg[\sum_{\mu\nu}K_{\mu i}(\mathbf{x}_0)K_{\nu j}(\mathbf{x}_0)\times\left(\left\langle\frac{\partial\chi_\mu(\mathbf{x})}{\partial b}\right|_{\mathbf{x}=\mathbf{x}_0}\Big|\chi_\nu(\mathbf{x}_0)\right\rangle-\left\langle\chi_\mu(\mathbf{x}_0)\left|\frac{\partial\chi_\nu(\mathbf{x})}{\partial b}\right|_{\mathbf{x}=\mathbf{x}_0}\right\rangle\right)\Bigg], \tag{21}$$

where we have used Eqs. (9) and (20). Note that this matrix is antisymmetric.

For the creation operators Eq. (17) leads to the identity

$$\frac{\partial a_i^\dagger(\mathbf{x})}{\partial b}=\sum_j D_{ji}^{(b)}(\mathbf{x})a_j^\dagger(\mathbf{x})+a_{\perp i}^\dagger(\mathbf{x}), \tag{22}$$

where $a_{\perp i}^\dagger(\mathbf{x})$ is the operator that creates an electron in $\varphi_{\perp i}(\mathbf{x})$. Thus,

$$[a_i(\mathbf{x}),a_{\perp j}^\dagger(\mathbf{x})]_+=\langle\varphi_i(\mathbf{x})\,|\,\varphi_{\perp j}(\mathbf{x})\rangle=0. \tag{23}$$

Using Eq. (22) in Eq. (15) gives

$$\frac{\partial}{\partial b}|\tilde{0}(\mathbf{x})\rangle|_{\mathbf{x}=\mathbf{x}_0}=\Bigg(\sum_{i>j}\kappa_{ij}^{(b)}(\mathbf{x}_0)q_{ij}^-(\mathbf{x}_0)+\sum_{r\neq0}P_r^{(b)}(\mathbf{x}_0)R_r^-(\mathbf{x}_0)+\sum_{i,j}^{\text{all}}D_{ij}^{(b)}(\mathbf{x}_0)q_{ij}(\mathbf{x}_0)+\sum_i a_{\perp i}^\dagger(\mathbf{x}_0)a_i(\mathbf{x}_0)\Bigg)|0(\mathbf{x}_0)\rangle. \tag{24}$$

The first sum on the right-hand side is only over nonredundant orbital rotations whereas the third sum is over *all* orbital rotations.

From Eq. (1) we see that FO-NACME involving a MCSCF reference state are formed by multiplying Eq. (24) from the left with other states. These states are spanned in the same one-electron basis as the reference state, and according to Eq. (23), the last term in Eq. (24) is not going to contribute. Therefore, for the purpose of calculating FO-NACME at a geometry $\mathbf{x}_0$, the first-order differentiation of the reference state with respect to a nuclear coordinate b corresponds to applying the operator

$$\hat{g}_0(\mathbf{x}_0,b)\equiv\sum_{i>j}\kappa_{ij}^{(b)}(\mathbf{x}_0)q_{ij}^-(\mathbf{x}_0)+\sum_{r\neq0}P_r^{(b)}(\mathbf{x}_0)R_r^-(\mathbf{x}_0)+\sum_{i,j}^{\text{all}}D_{ij}^{(b)}(\mathbf{x}_0)q_{ij}(\mathbf{x}_0). \tag{25}$$

Since the matrix $\mathbf{D}^{(b)}(\mathbf{x}_0)$ in Eq. (21) is antisymmetric, the operator $\hat{g}_0(\mathbf{x}_0,b)$ is anti-Hermitian, $\hat{g}_0^\dagger(\mathbf{x}_0,b)=-\hat{g}_0(\mathbf{x}_0,b)$. Note that the operator $\hat{g}_0(\mathbf{x}_0,b)$ is specific for the wave function upon which it acts.

B. Response theory calculations of FO-NACME

For exact states, the transition matrix elements between the reference state and orthogonal states for a general time-independent operator appear in the residues of linear response functions. For MCSCF reference states, the linear response functions have been derived and the transition matrix elements have been identified by comparing the MCSCF residues to those of the exact states. According to Eq. (5.97) of Ref. 10, this identification gives, for a general time independent operator A,

$$\langle n(\mathbf{x}_0)\,|A|\,0(\mathbf{x}_0)\rangle=\langle0(\mathbf{x}_0)\,|\,[O_n^\dagger(\mathbf{x}_0),A]\,|0(\mathbf{x}_0)\rangle. \tag{26}$$

The $O_n(\mathbf{x}_0)$ operators are defined by a transformation of the manifold of operators in eq. (6)

$$O_n(\mathbf{x}_0)=[T(\mathbf{x}_0)]\mathbf{X}_n(\mathbf{x}_0). \tag{27}$$

The $\mathbf{X}_n(\mathbf{x}_0)$ is the excitation vector and it is found as described in Ref. 10 by solving a generalized eigenvalue problem.

According to Eq. (25) the FO-NACME of interest in this work have the form

$$g_{n0}(\mathbf{x}_0,b)=\langle n(\mathbf{x}_0)\,|\,\hat{g}_0(\mathbf{x}_0,b)\,|0(\mathbf{x}_0)\rangle. \tag{28}$$

Using the identification in Eq. (26) of transition matrix elements for MCSCF states, this element is evaluated as

$$g_{n0}(\mathbf{x}_0,b)=\langle0(\mathbf{x}_0)\,|\,[O_n^\dagger(\mathbf{x}_0),\hat{g}_0(\mathbf{x}_0,b)]\,|0(\mathbf{x}_0)\rangle=\mathbf{C}^{(b)}(\mathbf{x}_0)^e\mathbf{S}^{[2]*}(\mathbf{x}_0)\mathbf{X}_n^*(\mathbf{x}_0)+{}^e\mathbf{D}^{(b)[1]^T}(\mathbf{x}_0)\mathbf{X}_n^*(\mathbf{x}_0). \tag{29}$$

The first term is called the wave-function response (WFR) term and the second term is called the basis-set response (BSR) term. The vector $\mathbf{C}^{(b)}(\mathbf{x}_0)$ is

$$\mathbf{C}^{(b)}(\mathbf{x}_0) \equiv [\kappa^{(b)}(\mathbf{x}_0) \quad P^{(b)}(\mathbf{x}_0) \quad -\kappa^{(b)}(\mathbf{x}_0) \quad -P^{(b)}(\mathbf{x}_0)]. \tag{30}$$

The row vectors $\kappa^{(b)}(\mathbf{x}_0)$ and $P^{(b)}(\mathbf{x}_0)$ contain the elements $\kappa_{ij}^{(b)}(\mathbf{x}_0)$ and $P_r^{(b)}(\mathbf{x}_0)$. For these elements $i>j$ and the sets refer to nonredundant orbital rotations only. The r index refers to all but the reference state in the configuration space. The matrix ${}^e\mathbf{S}^{[2]}(\mathbf{x}_0)$ is a generalized metric matrix which is defined in Eq. (5.64) of Ref. 10,

$${}^e\mathbf{S}^{[2]}(\mathbf{x}_0) \equiv \begin{pmatrix} \Sigma(\mathbf{x}_0) & \Delta(\mathbf{x}_0) \\ -\Delta(\mathbf{x}_0)^* & -\Sigma(\mathbf{x}_0)^* \end{pmatrix} \tag{31}$$

with

$$\Sigma(\mathbf{x}_0) \equiv \begin{pmatrix} \langle 0(\mathbf{x}_0)|[q_{ij}(\mathbf{x}_0),q_{kl}^\dagger(\mathbf{x}_0)]|0(\mathbf{x}_0)\rangle & \langle 0(\mathbf{x}_0)|[q_{ij}(\mathbf{x}_0),R_s^\dagger(\mathbf{x}_0)]|0(\mathbf{x}_0)\rangle \\ \langle 0(\mathbf{x}_0)|[R_r(\mathbf{x}_0),q_{kl}^\dagger(\mathbf{x}_0)]|0(\mathbf{x}_0)\rangle & \langle 0(\mathbf{x}_0)|[R_r(\mathbf{x}_0),R_s^\dagger(\mathbf{x}_0)]|0(\mathbf{x}_0)\rangle \end{pmatrix}, \tag{32a}$$

$$\Delta(\mathbf{x}_0) \equiv \begin{pmatrix} \langle 0(\mathbf{x}_0)|[q_{ij}(\mathbf{x}_0),q_{kl}(\mathbf{x}_0)]|0(\mathbf{x}_0)\rangle & \langle 0(\mathbf{x}_0)|[q_{ij}(\mathbf{x}_0),R_s(\mathbf{x}_0)]|0(\mathbf{x}_0)\rangle \\ \langle 0(\mathbf{x}_0)|[R_r(\mathbf{x}_0),q_{kl}(\mathbf{x}_0)]|0(\mathbf{x}_0)\rangle & \langle 0(\mathbf{x}_0)|[R_r(\mathbf{x}_0),R_s(\mathbf{x}_0)]|0(\mathbf{x}_0)\rangle \end{pmatrix}, \tag{32b}$$

and the vector ${}^e\mathbf{D}^{(b)[1]}(\mathbf{x}_0)$ is defined as ${}^e\mathbf{V}^{\omega_1[1]}$ in Eq. (5.48) of Ref. 10 with the operator $\hat{V}^{\omega_1}$ replaced by

$$\hat{D}^{(b)}(\mathbf{x}_0) \equiv \sum_{i,j}^{\text{all}} D_{ij}^{(b)}(\mathbf{x}_0) q_{ij}(\mathbf{x}_0). \tag{33}$$

That is

$${}^e\mathbf{D}^{(b)[1]}(\mathbf{x}_0) \equiv \begin{pmatrix} \langle 0(\mathbf{x}_0)|[q_{ij}(\mathbf{x}_0),\hat{D}^{(b)}(\mathbf{x}_0)]|0(\mathbf{x}_0)\rangle \\ \langle 0(\mathbf{x}_0)|[R_r(\mathbf{x}_0),\hat{D}^{(b)}(\mathbf{x}_0)]|0(\mathbf{x}_0)\rangle \\ \langle 0(\mathbf{x}_0)|[q_{ij}^\dagger(\mathbf{x}_0),\hat{D}^{(b)}(\mathbf{x}_0)]|0(\mathbf{x}_0)\rangle \\ \langle 0(\mathbf{x}_0)|[R_r^\dagger(\mathbf{x}_0),\hat{D}^{(b)}(\mathbf{x}_0)]|0(\mathbf{x}_0)\rangle \end{pmatrix}. \tag{34}$$

We have now completed the discussion on the evaluation of the FO-NACME in Eq. (29).

C. Alternative procedure for evaluating FO-NACME

The identification of the FO-NACME for general MCSCF wave functions in Eq. (26) is in agreement with MCSCF response theory for evaluating transition matrix elements for an operator, in this case $\hat{g}_0(\mathbf{x}_0,b)$. An alternative approach would be to postpone the identification of the effective operator for $\partial/\partial b$ until after the NACME have been identified from MCSCF response theory, that is

$$\begin{aligned} g_{n0}(\mathbf{x}_0,b) &= \left\langle \tilde{0}(\mathbf{x}) \middle| \left[O_n^\dagger(\mathbf{x}), \frac{\partial}{\partial b} \right] \middle| \tilde{0}(\mathbf{x}) \right\rangle \Big|_{\mathbf{x}=\mathbf{x}_0} \\ &= \left\langle \tilde{0}(\mathbf{x}) \middle| O_n^\dagger(\mathbf{x}) \frac{\partial}{\partial b} \middle| \tilde{0}(\mathbf{x}) \right\rangle \Big|_{\mathbf{x}=\mathbf{x}_0} \\ &\quad - \langle \tilde{0}(\mathbf{x}) | \frac{\partial}{\partial b} O_n^\dagger(\mathbf{x}) | \tilde{0}(\mathbf{x}) \rangle_{\mathbf{x}=\mathbf{x}_0}. \end{aligned} \tag{35}$$

$O_n(\mathbf{x})$ is defined for a general $\mathbf{x}$ in the same way as $O_n(\mathbf{x}_0)$ is defined for $\mathbf{x}_0$ in Eq. (27). The orbital and state transfer operators $[T(\mathbf{x})]$ refer to orbitals and states that are optimized at $\mathbf{x}$ according to Eq. (13). In the first term on the right-hand side of Eq. (35) the differentiation acts upon the reference wave function and we can therefore substitute it by $\hat{g}_0(\mathbf{x}_0,b)$. In the second term, however, the differentiation does not act directly on the reference state, but rather on the state created by applying the operator $O_n(\mathbf{x})$ on the reference state. Therefore, in this term the differentiation cannot be directly substituted by $\hat{g}_0(\mathbf{x}_0,b)$.

For FCI and CAS-MCSCF reference wave functions, the expectation values of the operators contained in $[T(\mathbf{x})]$ are zero

$$\langle \tilde{0}(\mathbf{x}) | O_n^\dagger(\mathbf{x}) | \tilde{0}(\mathbf{x}) \rangle = 0. \tag{36}$$

Differentiating this condition with respect to b gives for $\mathbf{x}=\mathbf{x}_0$,

$$\begin{aligned} &\left\langle \tilde{0}(\mathbf{x}) \middle| \frac{\partial}{\partial b} O_n^\dagger(\mathbf{x}) \middle| \tilde{0}(\mathbf{x}) \right\rangle \Big|_{\mathbf{x}=\mathbf{x}_0} \\ &= - \left\langle \tilde{0}(\mathbf{x}) \middle| O_n(\mathbf{x}) \frac{\partial}{\partial b} \middle| \tilde{0}(\mathbf{x}) \right\rangle^* \Big|_{\mathbf{x}=\mathbf{x}_0} \\ &= - \langle 0(\mathbf{x}_0) | \hat{g}_0^\dagger(\mathbf{x}_0,b) O_n^\dagger(\mathbf{x}_0) | 0(\mathbf{x}_0) \rangle. \end{aligned} \tag{37}$$

As noted previously the operator $\hat{g}_0(\mathbf{x}_0,b)$ is anti-Hermitian. Therefore, Eq. (37) can be used in Eq. (35) with the result

$$\begin{aligned} g_{n0}(\mathbf{x}_0,b) &= \langle 0(\mathbf{x}_0) | O_n^\dagger(\mathbf{x}_0) \hat{g}_0(\mathbf{x}_0,b) | 0(\mathbf{x}_0) \rangle \\ &\quad - \langle 0(\mathbf{x}_0) | \hat{g}_0(\mathbf{x}_0,b) O_n^\dagger(\mathbf{x}_0) | 0(\mathbf{x}_0) \rangle. \end{aligned} \tag{38}$$

which is identical to Eq. (29).

The assumption used when deriving Eq. (38) is that the wave functions obey Eq. (36). This is not the case for wave functions constructed as restricted active space

TABLE I. Electronic energies of the $\underline{B}$, B', and $B''\overline{B}$ (1, 2, and 3 $^1\Sigma_u^+$) states and the FO-NACME ($g_{B'B}=\langle B'|\partial/\partial R|B\rangle$ and $g_{B''\overline{B}B}=\langle B''\overline{B}|\partial/\partial R|B\rangle$) in various calculations (Calc.) at three internuclear distances R. All values are listed in atomic units.

R(H–H)	Calc.	B energy	B' energy	$B''\overline{B}$ energy	$g_{B'B}$	$g_{B''\overline{B}B}$
3.0	200	−0.741 070	−0.646 306	−0.613 273	0.103 134	0.051 183
	210	−0.749 166	−0.648 041	−0.613 884	0.101 069	0.049 458
	310	−0.750 323	−0.648 656	−0.614 732	0.100 708	0.050 008
	631	−0.751 662	−0.649 207	−0.615 241	0.100 906	0.050 525
	FCI	−0.751 754	−0.649 251	−0.615 292	0.100 884	0.050 583
	W&D[a]	−0.752 526	−0.649 502	−0.615 598[b]	0.100 416	
5.0	200	−0.701 560	−0.624 617	−0.568 780	0.052 625	0.045 279
	210	−0.710 348	−0.625 226	−0.569 204	0.044 917	0.044 954
	310	−0.712 224	−0.625 627	−0.571 860	0.046 159	0.044 560
	631	−0.713 834	−0.626 399	−0.573 682	0.044 408	0.043 784
	FCI	−0.713 947	−0.626 495	−0.573 976	0.044 366	0.043 612
	W&D[a]	−0.714 851	−0.626 634	−0.574 076[c]	0.043 428	
8.0	200	−0.652 928	−0.625 314	−0.578 457	0.021 653	0.063 279
	210	−0.658 718	−0.625 428	−0.582 947	0.021 753	0.045 884
	310	−0.660 172	−0.625 394	−0.589 580	0.017 063	0.040 492
	631	−0.661 419	−0.625 767	−0.591 293	0.014 646	0.037 236
	FCI	−0.661 514	−0.625 795	−0.591 486	0.014 718	0.036 945
	W&D[a]	−0.662 434	−0.625 871	−0.592 761	0.013 083	

[a]Reference 8(a).
[b]Reference 17.
[c]Reference 16.

(RAS) MCSCF wave functions. However, the RAS wave functions used in practice are extended CAS functions and deviate only slightly from the corresponding CAS functions. For usual RAS-MCSCF wave functions we therefore expect that Eq. (29) can be used for evaluating FO-NACME as also suggested by the derivation leading to Eq. (29). Furthermore, notice that for FCI wave functions, Eq. (29) represents the exact results. When CAS and RAS wave functions are extended toward the FCI limit, the FO-NACME calculated by Eq. (29) are therefore expected to converge in a similar fashion toward the exact FCI results.

III. CALCULATIONS

To investigate the efficiency and the accuracy of the described method, we present sample calculations for $^1\Sigma_u^+$ states of H_2, $^3B_2$ states of MgH_2, and $^1\Sigma^+$ states of

TABLE II. Occupancies of natural orbitals for the B state obtained at three internuclear distances from FCI calculations. The distances are in atomic units and the symmetry (Sym.) of the orbitals are listed according to the $D_{\infty h}$ point group.

R(H–H)	Sym.	Occupancies				
3.0	σ_g and σ_u	0.98×10^{-0}	0.98×10^{-2}	0.52×10^{-3}	0.75×10^{-4}	0.26×10^{-4}
		0.87×10^{-5}	0.25×10^{-5}	0.13×10^{-5}	0.31×10^{-6}	0.12×10^{-6}
		0.26×10^{-7}	0.2×10^{-8}	$<1\times10^{-9}$	$<1\times10^{-9}$	$<1\times10^{-9}$
	π_g and π_u	0.31×10^{-2}	0.67×10^{-4}	0.23×10^{-4}	0.42×10^{-5}	0.28×10^{-6}
		$<1\times10^{-9}$	$<1\times10^{-9}$			
	δ_g and δ_u	0.53×10^{-4}				
5.0	σ_g and σ_u	0.97×10^{-0}	0.18×10^{-1}	0.12×10^{-2}	0.12×10^{-3}	0.49×10^{-4}
		0.21×10^{-4}	0.57×10^{-5}	0.22×10^{-5}	0.61×10^{-6}	0.21×10^{-6}
		0.12×10^{-6}	0.12×10^{-7}	$<1\times10^{-9}$	$<1\times10^{-9}$	$<1\times10^{-9}$
	π_g and π_u	0.40×10^{-2}	0.78×10^{-4}	0.48×10^{-4}	0.42×10^{-5}	0.70×10^{-6}
		$<1\times10^{-9}$	$<1\times10^{-9}$			
	δ_g and δ_u	$.53\times10^{-4}$				
8.0	σ_g and σ_u	0.97×10^{-0}	0.24×10^{-1}	0.14×10^{-2}	0.14×10^{-3}	0.38×10^{-4}
		0.31×10^{-4}	0.61×10^{-5}	0.18×10^{-5}	0.61×10^{-6}	0.21×10^{-6}
		0.83×10^{-7}	0.50×10^{-7}	0.12×10^{-7}	$<1\times10^{-9}$	$<1\times10^{-9}$
	π_g and π_u	0.33×10^{-2}	0.65×10^{-4}	0.36×10^{-4}	0.35×10^{-5}	0.68×10^{-6}
		1×10^{-9}	$<1\times10^{-9}$			
	δ_g and δ_u	0.35×10^{-4}				

TABLE III. Number of active orbitals for the CAS termed 200, 210, 310, and 631, and FCI. The orbital symmetries are listed according to the $D_{\infty h}$ point group.

Designation	σ_g	π_g	δ_g	σ_u	π_u	δ_u
200	2	0	0	2	0	0
210	2	1	0	2	1	0
310	3	1	0	3	1	0
631	6	3	1	6	3	1
FCI	15	7	1	15	7	1

BH. The results are compared with previously reported results using other methods. All the calculations were performed with the SIRIUS–ABACUS–RESPONS program system[14] which was augmented with the necessary code to calculate FO-NACME according to the theory of the previous section.

A. The three lowest $^1\Sigma_u^+$ states of H_2

The FO-NACME of Wolniewicz and Dressler[8a] for the B and B' $^1\Sigma_u^+$ states of H_2 represent the most accurate NACME for two-electron systems. We have, for comparison, carried out calculations on this system. We further report NACME between the B and $B''\overline{B}$ $^1\Sigma_u^+$ states.

We used the Cartesian Gaussian basis set 20A of Augspurger and Dykstra[15] where the d exponent was altered to 0.4 and augmented with two diffuse s (α=0.020 246 and 0.00 6749) and three diffuse p (α=0.05, 0.016 667, and 0.005 556) functions. This gives a (9s6p1d/7s6p1d) basis set on each H and a total of 62 contracted basis functions for the H_2 system. In Table I we report FCI calculations of total energies and FO-NACME for three internuclear distances (3.0, 5.0, and 8.0 a.u.) together with the corresponding values of Wolniewicz and Dressler.[8a] The FO-NACME are calculated with respect to the coordinate representing the internuclear distance. It is seen that energies differ by less than 1 mH, and the FO-NACME by less than 0.0017 a.u. emphasizing the adequacy of the basis.

The occupancies of natural orbitals (NO) as obtained in the FCI calculations for the B state are given in Table II. These occupancies measure the importance of the NO in the electronic wave function and may be used to choose the CAS in the MCSCF calculations. We have selected four different CAS designations, 200, 210, 310, and 631, with 4, 8, 10, and 28 active orbitals. The symmetry of the orbitals in the CAS is given in Table III. The symmetry is listed according to the molecular point group, $D_{\infty h}$, but the calculations were performed in the subgroup D_{2h}. The MCSCF calculations were carried out for the B state at three internuclear distances as reported in Table I and response theory was used to calculate the excitation energies and the FO-NACME from the B to the B' and $B''\overline{B}$ states.

Even the small 200 CAS calculation is in good qualitative agreement with the FCI results. The discrepancies are reduced when we go to the 210 CAS, and for the 310 CAS the energy is within 2 mH of the FCI results and the NACME differ by less than 0.005 a.u. The 631 CAS calculations reproduce the FCI results and we have chosen this wave function for a set of calculations covering the whole range of internuclear distances from 1.2 to 10 a.u.

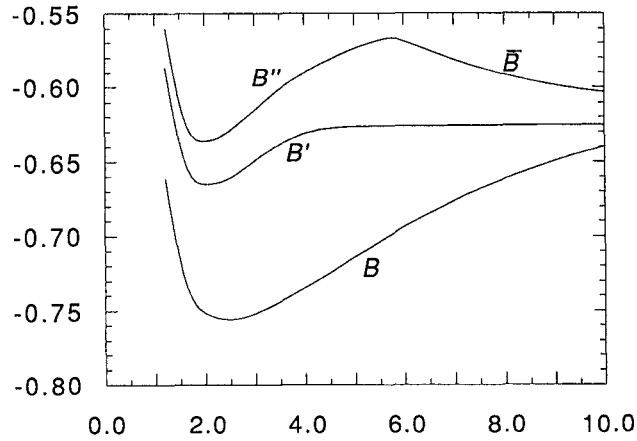

FIG. 1. The three lowest $^1\Sigma_u^+$ potentials of H_2. Energy and internuclear distance in atomic units.

The potential-energy curves obtained for the B, B', and $B''\overline{B}$ states are plotted in Fig. 1. The largest discrepancies to the best published values[8a,16,17] are 1.1 mH for the B state, 0.3 mH for the B' state, and 2.2 mH for the $B''\overline{B}$ state. As discussed elsewhere,[18] the B state is dominated by the $1s\sigma_g$, $2p\sigma_u$ electronic configuration and dissociates to H(1s)+H(2p). Around its equilibrium distance the B' state is primarily a $1s\sigma_g$, $3p\sigma_u$ state but it dissociates to H(1s)+H(2s). The $B''\overline{B}$ state is dominated by $1s\sigma_g$, $4p\sigma_u$ in the inner region. It has a sharp avoided crossing with the fourth $^1\Sigma_u^+$ state around 5.75 a.u. It becomes an ionic state which crosses the H(1s)+H(n=2) state at 39 a.u.[16] The $B''\overline{B}$ state therefore dissociates into H(1s)+H(n=2).

In Fig. 2 the FO-NACME $g_{B'B}$ for the B and B' states are compared to the essentially exact results of Wolniewicz and Dressler.[8a] The agreement is excellent. The largest discrepancy is 0.0018 a.u. which is 1.2% of the maximum value of 0.1434 a.u. at 2.0 a.u.

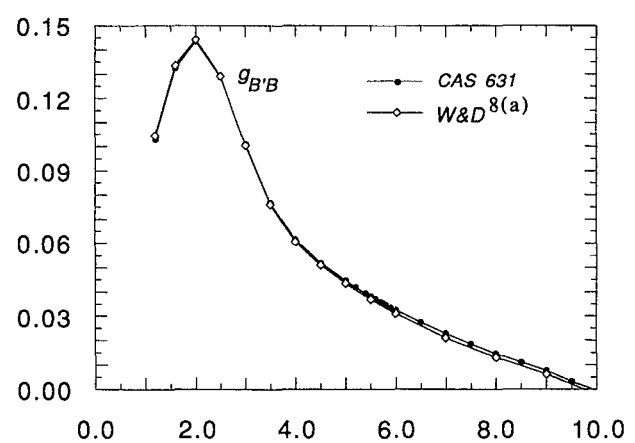

FIG. 2. FO-NACME between the B and B' $^1\Sigma_u^+$ states of H_2 ($g_{B'B}$ $=\langle B'|\partial/\partial R|B\rangle$) as a function of the internuclear distance R. Units in atomic units.

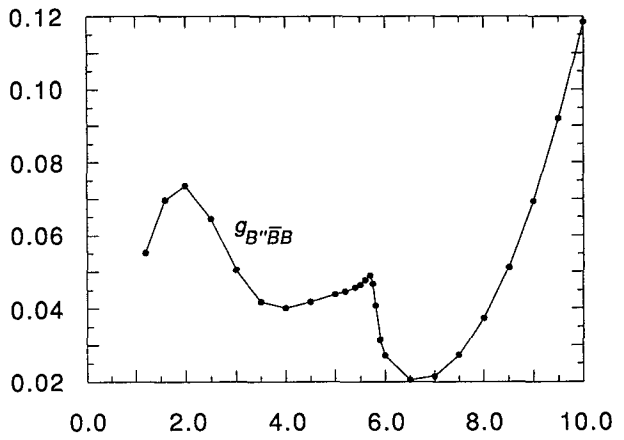

FIG. 3. FO-NACME between the B and $B''\bar{B}$ $^1\Sigma_u^+$ states of H_2 ($g_{B''BB} = \langle B''\bar{B}|\partial/\partial R|B\rangle$) as a function of the internuclear distance R. Units in atomic units.

In Fig. 3 the FO-NACME $g_{B''\bar{B}B}$ for the B and $B''\bar{B}$ states are plotted. These elements were obtained simultaneously with the $g_{B'B}$ coupling elements. The $B''\bar{B}$ energies are of the same quality as the B' energies. Therefore, we expect the $g_{B''\bar{B}B}$ NACME to be of the same quality as the $g_{B'B}$ elements. The $g_{B''\bar{B}B}$ curve has a complicated structure. The first peak occurs around 2.0 a.u. At 5.7 a.u., the curve looks almost indifferentiable. The rapid change in the coupling elements at this point is due to the sharp avoided crossing that occur for the $B''\bar{B}$ state at this geometry. The $g_{B''\bar{B}B}$ has a minimum at 6.5 a.u. and raises thereafter as the B and $B''\bar{B}$ potentials approach each other for larger bond lengths.

The FO-NACME in Eq. (29) are a sum of two contributions, the first is the WFR term and the second is the BSR term. In Fig. 4 the $g_{B'B}$ function is plotted together with the two individual contributions. For smaller internuclear distances the individual contributions are numerically considerably larger than the coupling elements themselves. The relationship between the WFR and BSR terms can be altered by changing the orbital connection. However, the

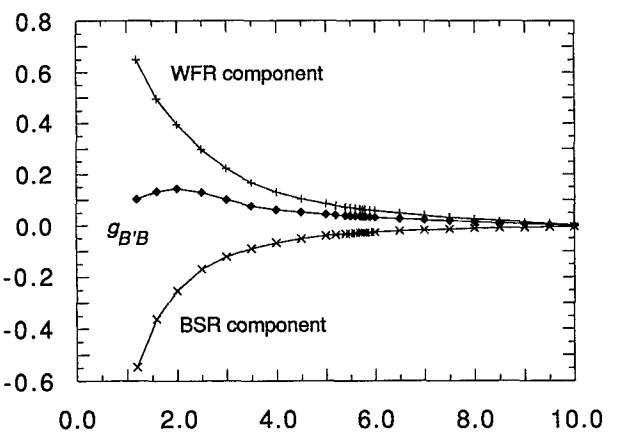

FIG. 4. FO-NACME between the B and B' $^1\Sigma_u^+$ states of H_2 and the two components (WFR and BSR) of which it is a sum. Units in atomic units.

$S^{-1/2}(\mathbf{x})$ connection employed in this work does not appear to give any numerical instability problems in the present calculations.

B. The two lowest $^3B_2$ states of MgH_2

Lengsfield, Saxe, and Yarkony[9a] have used state-averaged MCSCF theory to calculate the FO-NACME between the first and second $^3B_2$ surfaces of MgH_2 in C_{2v} symmetry. The H–H distance was kept fixed at 2.50 a.u. For comparison we carried out calculations for the same system using the same basis and the same active orbitals. The basis is a small Cartesian Gaussian basis of 28 functions, and four electrons were distributed in the four active orbitals ($4a_1$, $5a_1$, $2b_2$, $3b_2$). The $1\,^3B_2$ state was used as reference state in our calculations.

The total energies and NACME are given in Table IV together with the SA-MCSCF results of Lengsfield *et al.*[9a] As our $1\,^3B_2$ potential is fully optimized in the CAS-MCSCF calculation, it is at all points slightly lower than the corresponding SA-MCSCF $1\,^3B_2$ potential. For R(Mg–H_2) less than 4.5 a.u. the $2\,^3B_2$ potential curve we calculated is lower than the SA-MCSCF potential. For R(Mg–H_2) larger than 4.5 a.u. the opposite is true.

There are three totally symmetric internal coordinates (z_{Mg}, $z_H = z_{H1} + z_{H2}$, and $y_H = y_{H1} - y_{H2}$) for MgH_2 in C_{2v} symmetry. Three sets of FO-NACME [$g_{21}(z_{Mg})$, $g_{21}(z_H)$, and $g_{21}(y_H)$] can therefore be calculated between the $1\,^3B_2$ and $2\,^3B_2$ states. The wave functions $1\,^3B_2$ and $2\,^3B_2$ are only determined within an arbitrary phase factor and the g_{21} coupling elements are therefore also arbitrary within a phase factor. However, if the phase of one g_{21} element is chosen, say the phase of $g_{21}(z_{Mg})$, then the phases of the other elements $g_{21}(z_H)$ and $g_{21}(y_H)$ are fixed. From Table IV it is seen that the $g_{21}(z_{Mg})$ and $g_{21}(z_H)$ elements of this work and of Ref. 9(a) agree fairly well, while the $g_{21}(y_H)$ elements only agrees within a sign. We are confident that the sign of our $g_{21}(y_H)$ elements is correct relative to the signs of $g_{21}(z_{Mg})$ and $g_{21}(z_H)$ and believe that the sign of the SA-MCSCF $g_{21}(y_H)$ elements is incorrect in Ref. 9(a). In Fig. 5 we have plotted the FO-NACME results of Table IV, but we have changed the sign of the SA-MCSCF $g_{21}(y_H)$ elements. The results are similar.

C. The three lowest $^1\Sigma^+$ states of BH

Several *ab initio* calculations have been performed on the BH system. Jaszunski, Roos, and Widmark[19] have calculated accurate potential curves for the $X\,^1\Sigma^+$ ground state and the first excited $B\,^1\Sigma^+$ state. From these they have calculated the vibrational spectra, which agree within 3.5 cm^{-1} for the ground state and within 22 cm^{-1} for the B state.

In the course of this work we were informed about recent calculations of FO-NACME for the BH system by Cimiraglia.[12] Cimiraglia used the CIPSI (configuration interaction by perturbation with multiconfigurational zeroth-order wave function selected by iterative process) technique to generate both adiabatic and diabatic electronic wave functions. A finite difference technique was used to

TABLE IV. Energies for, and FO-NACME between, the 1 and 2 $^3B_2$ states of MgH_2. The coordinates z_H and y_H are defined as $z_H = z_{H1} + z_{H2}$ and $y_H = y_{H1} - y_{H2}$. We give in parentheses the SA-MCSCF values by Lengsfield, Saxe, and Yarkony [Ref. 9(a)]. All values are in atomic units.

$R(Mg-H_2)$[a]	$1\,^3B_2$ energy	$2\,^3B_2$ energy	$g_{21}(z_{Mg})$	$g_{21}(z_H)$	$g_{21}(y_H)$
2.0	−200.466 138	−200.274 375	0.045	−0.003	0.072
	(−200.458 881	−200.228 046	0.159	−0.033	−0.136)
2.5	−200.588 664	−200.396 421	−0.081	0.030	0.195
	(−200.581 927	−200.382 190	−0.182	0.034	−0.193)
3.0	−200.628 954	−200.469 084	−0.171	0.054	0.293
	(−200.622 723	−200.457 101	−0.209	0.052	−0.266)
3.5	−200.633 175	−200.507 815	−0.250	0.095	0.426
	(−200.627 304	−200.495 130	−0.263	0.093	−0.361)
4.0	−200.624 958	−200.525 519	−0.341	0.148	0.566
	(−200.619 771	−200.515 962	−0.297	0.130	−0.489)
4.5	−200.615 912	−200.528 796	−0.333	0.155	0.573
	(−200.611 910	−200.527 245	−0.257	0.123	−0.548)
5.0	−200.610 015	−200.526 245	−0.249	0.120	0.440
	(−200.606 623	−200.532 921	−0.208	0.104	−0.473)
5.5	−200.606 851	−200.521 656	−0.158	0.079	0.283
	(−200.603 606	−200.535 400	−0.150	0.076	−0.339)
6.0	−200.605 201	−200.517 867	−0.092	0.167	0.048
6.5	−200.604 270	−200.515 603	−0.052	0.095	0.027
7.0	−200.603 673	−200.514 453	−0.028	0.054	0.016

[a]Mg, H1, and H2 are located at [0, 0, $R(Mg-H_2)$], (0, 1.25, 0), and (0, −1.25, 0), respectively.

calculate the FO-NACME for the adiabatic wave functions. For the diabatic functions the coupling elements were estimated by interpolation of an effective Hamiltonian. The NACME calculated with the two methods are very similar.

Cimiraglia used the diabatic representation to discuss the dominant electronic configurations of the adiabatic states.[12] The X state is for all internuclear distances $B(^2P;2s^2,2p)$ $H(^2S;1s)$. The B state dissociates to $B(^2S;2s^2,3s)+H(^2S;1s)$. In the outer well (see Fig. 6) it has a strong ionic character B^+H^- and in the inner well it is again dominated by the configuration $B(^2S;2s^2,3s)$ $H(^2S;1s)$. The C state dissociates into $B(^2D;2s,2p^2)$ $+H(^2S;1s)$. From the avoided crossing with the B state at 11 a.u. and until 18 a.u. the C state has a mixed character of B^+H^- and $B(^2P;2s^2,3p)$ $H(^2S;1s)$. From 4 a.u. and until 11 a.u. we assume the C state to have substantial $B(^2S;2s^2,3s)$ $H(^2S;1s)$ character and inside 4 a.u. it regains $B(^2D;2s,2p^2)$ $H(^2S;1s)$ as the dominant configuration.

We have performed FO-NACME calculations between the X and B states, and between the B and C states. For both B and H we have used the *pVDZ* correlation consistent basis set[20] augmented with diffuse functions. For B we added one s ($\alpha=0.034\,77$) and one p function ($\alpha=0.031\,79$), and for H one s ($\alpha=0.040\,67$). FCI calculations were carried out for the total energy and the FO-NACME at three internuclear distances (3.0, 7.0, and 10.0 a.u.). The natural orbitals obtained for the B state at these geometries are given in Table V. Based on these we have chosen three CAS spaces all containing the four valence electrons. These CAS spaces are termed 1251, 830, and 410

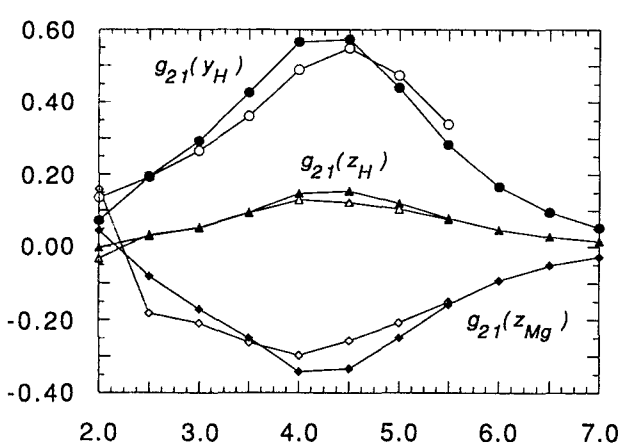

FIG. 5. FO-NACME between the 1 and 2 $^3B_2$ states of MgH_2 as a function of the Mg–H_2 distance ($g_{21}(x)=\langle 2|\partial/\partial x|1\rangle$). The H–H distance is kept fixed at 2.5 a.u. MgH_2 have C_{2v} symmetry and the Mg–H_2 distance is measured from Mg to the center of mass of H_2. The solid points are determined in this work and the open points by Lengsfield, Saxe, and Yarkony [Ref. 9(a)]. Units in atomic units.

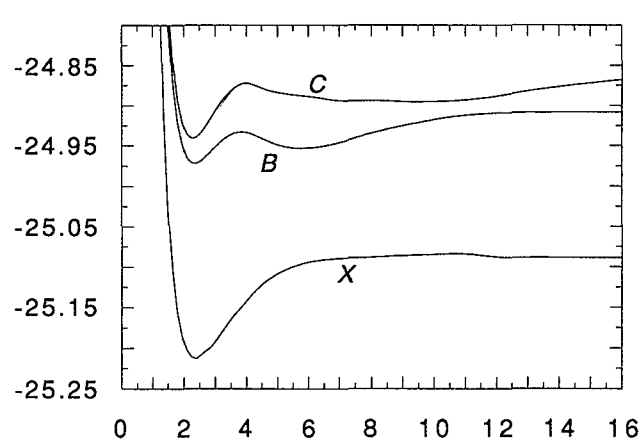

FIG. 6. The three lowest $^1\Sigma^+$ potentials of BH as obtained in the 830 CAS calculations. Energy and internuclear distance in atomic units.

TABLE V. Occupancies of natural orbitals obtained for the $B\,^1\Sigma^+$ state of BH at three internuclear distances from FCI calculations. The symmetry (Sym.) of the orbitals is listed according to the $C_{\infty v}$ point group. R(B–H) in atomic units.

R(B–H)	Sym.	Occupancies				
3.0	σ	1.9998	1.89	0.997	0.94	0.44×10^{-1}
		0.58×10^{-2}	0.32×10^{-2}	0.15×10^{-2}	0.91×10^{-3}	0.58×10^{-3}
		0.96×10^{-4}	0.78×10^{-4}	0.21×10^{-4}		
	π	0.51×10^{-1}	0.32×10^{-2}	0.27×10^{-2}	0.23×10^{-3}	0.15×10^{-3}
	δ	0.21×10^{-3}				
7.0	σ	1.9998	1.89	1.83	0.11	0.46×10^{-1}
		0.28×10^{-2}	0.20×10^{-2}	0.10×10^{-2}	0.66×10^{-3}	0.23×10^{-3}
		0.20×10^{-3}	0.75×10^{-4}	0.44×10^{-4}		
	π	0.58×10^{-1}	0.11×10^{-2}	0.79×10^{-3}	0.30×10^{-3}	0.55×10^{-4}
	δ	0.15×10^{-3}				
10.0	σ	1.9998	1.84	1.74	0.25	0.55×10^{-1}
		0.21×10^{-2}	0.12×10^{-2}	0.76×10^{-3}	0.51×10^{-3}	0.20×10^{-3}
		0.11×10^{-3}	0.64×10^{-4}	0.36×10^{-4}		
	π	0.58×10^{-1}	0.17×10^{-2}	0.48×10^{-3}	0.20×10^{-3}	0.79×10^{-4}
	δ	0.17×10^{-3}				

where, for example, the 1251 CAS has twelve active σ orbitals (2σ to 13σ), five active π orbitals (1π to 5π), and one active δ orbital (1δ). Although the symmetry labels refer to the $C_{\infty v}$ point group, our calculations are performed in the subgroup C_{2v}.

Table VI contains the energies and NACME obtained by the FCI and CAS calculations. We see that both energies and NACME uniformly approach the FCI values as the CAS is extended. At the 830 level, energies agree with FCI values within 8 mH except for the $C\,^1\Sigma^+$ energy at 3.00 a.u. which is 24 mH too high. Moreover, at the 830 level the FO-NACME agree well with the FCI results except for the coupling between the B and $C\,^1\Sigma^+$ states at 3.00 a.u. Knowing that for shorter internuclear distances discrepancies may arise for the C potential and the g_{CB} function, we have chosen to calculate potentials and couplings at the 830 level. In total we calculated 39 points for the curves, 16 of which are listed in Table VII. Calculations at the 1251 level were also carried out to allow for an extended examination of the g_{XB} and g_{CB} NACME functions. The potentials from the 830 calculations are displayed in Fig. 6 and the FO-NACME from both the 830 and 1251 calculations are plotted in Figs. 7 and 8. Note that the FO-NACME (g_{XB} and g_{CB}) listed in Table VII and shown in Figs. 7 and 8 are calculated with respect to the internuclear distance and with the center of mass fixed. The couplings apply to the isotope $^{11}B^1H$.

The g_{XB} functions found at the two levels of calculations are almost identical. The g_{XB} function has two extrema. The large appears around 2.75 a.u. close to the equilibrium distances of both the X and B states. The second extremum appears at 5.75 a.u., where the bottom of the second well of the B potential is found. The g_{XB} function is quite smooth, but the CAS 830 points at 2.4 and 2.6 a.u. are slightly off. The corresponding 1251 points do not exhibit similar displacements, however, the 1251 point in between at 2.5 a.u. is also displayed but in opposite direction. Although the calculations at these points are, as elsewhere, converged to 1×10^{-4}, the inconsistency between the two levels of calculations indicate that the displace-

TABLE VI. Electronic energies of the X, B, and C (1, 2, and $3\,^1\Sigma^+$) states and FO-NACME in various calculations (Calc.) for three internuclear distances R. The FO-NACME are calculated with respect to the z coordinate of both B (z_B) and H (z_H). The internuclear axis lies along the z direction. All values in atomic units.

R(B–H)	Calc.	X energy	B energy	C energy	$g_{XB}(z_B)$	$g_{XB}(z_H)$	$g_{CB}(z_B)$	$g_{CB}(z_H)$
3.0	410	−25.159 967	−24.933 847	−24.882 426	0.183	0.148	0.404	−0.225
	830	−25.192 012	−24.951 751	−24.906 272	0.086	0.256	0.225	−0.111
	1251	−25.194 763	−24.954 548	−24.927 978	0.082	0.254	0.000	−0.015
	FCI	−25.196 509	−24.956 226	−24.930 270	0.081	0.254	0.006	−0.020
7.0	410	−25.057 032	−24.936 958	−24.884 082	0.197	−0.060	0.092	0.059
	830	−25.089 306	−24.946 221	−24.894 004	0.188	−0.037	0.104	0.034
	1251	−25.092 156	−24.947 698	−24.894 031	0.182	−0.036	0.102	0.037
	FCI	−25.093 814	−24.949 018	−24.895 369	0.182	−0.036	0.102	0.037
10.0	410	−25.054 317	−24.912 228	−24.889 666	0.126	−0.005	0.260	−0.149
	830	−25.084 442	−24.917 232	−24.895 144	0.135	−0.004	0.275	−0.167
	1251	−25.090 490	−24.919 576	−24.897 646	0.129	−0.004	0.264	−0.160
	FCI	−25.092 167	−24.920 868	−24.898 948	0.129	−0.003	0.264	−0.160

TABLE VII. Electronic energies and FO-NACME calculated at various internuclear distances at the 830 CAS level for the X, B, and $C\,^1\Sigma^+$ states of BH. The FO-NACME are determined with the center of mass fixed. The atomic masses used are $M(^1\mathrm{H}) = 1.0078$ a.u. and $M(^{11}\mathrm{B}) = 11.0093$ a.u. All values in atomic units.

R(B–H)	X energy	B energy	C energy	g_{XB}	g_{CB}
1.2	−24.730 99	−24.495 23	−24.471 89	−0.096	−0.085
2.0	−25.193 74	−24.956 64	−24.928 17	−0.191	0.200
3.0	−25.192 01	−24.951 75	−24.906 27	−0.227	0.121
4.0	−25.141 57	−24.933 60	−24.871 79	−0.092	−0.225
5.0	−25.108 67	−24.949 01	−24.883 72	0.048	−0.179
6.0	−25.093 94	−24.952 87	−24.888 60	0.073	−0.071
7.0	−25.089 31	−24.946 22	−24.894 00	0.050	−0.022
8.0	−25.087 73	−24.934 44	−24.893 99	0.028	0.021
9.0	−25.085 75	−24.925 08	−24.895 18	0.020	0.085
10.0	−25.084 44	−24.917 23	−24.895 14	0.015	0.176
11.0	−25.083 91	−24.911 88	−24.893 15	0.014	0.229
12.0	−25.087 58	−24.909 36	−24.888 45	0.014	0.164
13.0	−25.088 07	−24.908 55	−24.881 89	0.014	0.088
14.0	−25.088 12	−24.908 15	−24.876 58	0.014	0.053
15.0	−25.088 14	−24.907 98	−24.871 75	0.014	0.034
16.0	−25.088 15	−24.907 91	−24.867 73	0.014	0.024

ments do not reflect a true feature of the g_{XB} function, but rather an instability in the response B to X deexcitation operator. This explanation is corroborated by the fact that we were not able to find a B to X deexcitation operator at the 830 level at 2.5 a.u.

Before analyzing and comparing the CAS 830 and CAS 1251 g_{CB} coupling functions, let us note that the 1251 function is in qualitative agreement with that of Cimiraglia.[12] The 830 and 1251 g_{CB} functions displayed in Fig. 8 are quite similar in the region from 4.0 a.u. and out. The two functions have four coinciding extrema and the two most outer ones are found in this region at 4.25 and 11.0 a.u. The one at 11.0 a.u. corresponds nicely to the avoided crossing between the B and C states at this geometry. Moreover, in the inner region between 1.2 and 3.5 a.u. the structure of the two functions is the same although they

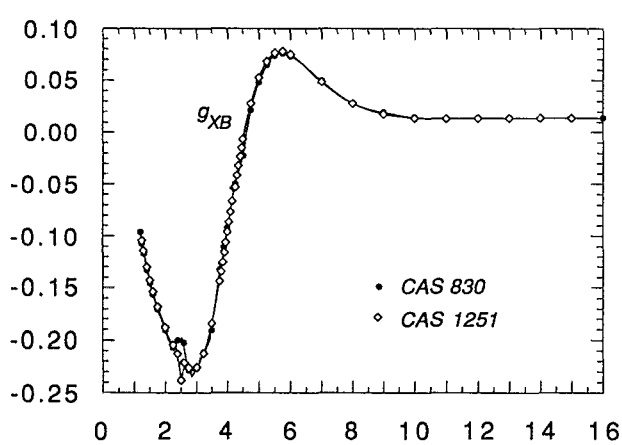

FIG. 7. FO-NACME between the X and $B\,^1\Sigma^+$ states of BH ($g_{XB} = \langle X|\partial/\partial R|B\rangle$) as a function of the internuclear distance R. Units in atomic units.

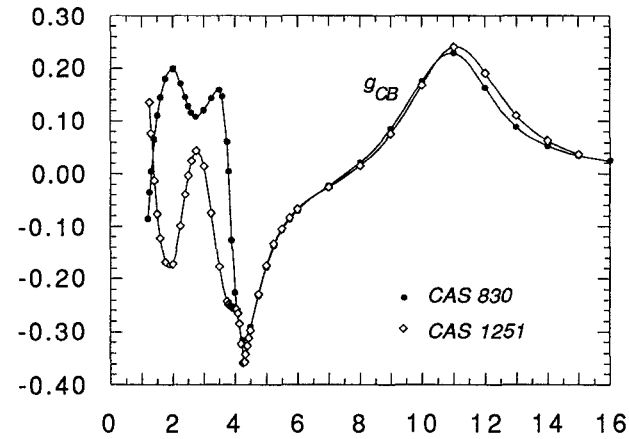

FIG. 8. FO-NACME between the C and $B\,^1\Sigma^+$ states of BH ($g_{CB} = \langle C|\partial/\partial R|B\rangle$) as a function of the internuclear distance R. Units in atomic units.

differ by a sign. In this region two extrema are found at 2.0 and 2.75 a.u. In contrast to the 1251 g_{CB} function the 830 g_{CB} function has a maximum at 3.5 a.u. and the main difference between the two functions is that the 830 function changes sign between 3.5 and 4.0 a.u. This does *not* happen for the 1251 function.

The performance of the 830 CAS calculation can be understood on the basis of the character of the X, B, and the C states. For the internuclear distances considered, the dominating electronic configurations of the reference state B differs from the dominating electronic configurations of the ground state by 1 orbital, and from the dominating electronic configurations of the C state also by 1 orbital except in the region inside 4.0 a.u. where it differs by 2. The operator manifold in Eq. (6) contains only one-electron excitations and deexcitations beside the state-transfer operators. Therefore, the orbital operators cannot create doubly-excited states from the dominant electron configuration of the reference state. The set of state-transfer operators, the CAS space, in such a case has to make up for this deficiency. In our calculations the 830 CAS, obviously, has not been large enough to ensure the C state to be well represented in the response calculation for small internuclear distances.

IV. SUMMARY

We have derived an analytic expression [Eq. (29)] that allows FO-NACME to be calculated. To obtain FO-NACME we first calculate the reference MCSCF state. Next the geometrical response of this state and the response vector defining the coupled state are obtained. In this process we also obtain excitation energy for the second state relative to the reference state. Thus, the method simultaneously provides FO-NACME as well as the potentials of the coupled states.

The results of the calculations on H_2, MgH_2, and BH are encouraging. The calculations of the $g_{B'B}$ coupling for H_2 demonstrate that very accurate results can be obtained with a reasonable basis and a limited CAS. Also, the $g_{B''\bar{B}B}$

function was obtained for H_2. For MgH_2, a small CAS calculation of FO-NACME between the 1 and 2 $^3B_2$ states was compared to a corresponding SA-MCSCF calculation, giving similar results.

The BH calculations show that the calculated FO-NACME converge towards FCI as the CAS is expanded. A limited CAS calculation gives good quantitative results for the g_{XB} coupling function and also for g_{CB} for internuclear distances above 4.0 a.u. For smaller distances it is clear that a larger CAS is needed since, in this region, the electron distributions of the dominating electronic configurations of B and C states, differ by two orbitals rather than just one.

ACKNOWLEDGMENTS

We would like to thank Dr. Cimiraglia for providing us with a preprint of Ref. 12 before publication. This work has been supported by the Danish Natural Science Research Council (Grant No 11-9004) and Nordisk Forskeruddannelsesakademi.

[1] M. Born and R. Oppenheimer, Ann. Phys. (Leipzig) **84**, 457 (1927).
[2] P. Senn, P. Quadrelli, and K. Dressler, J. Chem. Phys. **89**, 7401 (1988).
[3] K. L. Bak and J. Linderberg, J. Chem. Phys. **92**, 3668 (1990).
[4] *Advances in Chemical Physics*, edited by M. Baer and C. Y. Ng (Wiley, New York, 1992), Vol. 82.
[5] L. D. Landau, Phys. Zeit. Sowjet. **2**, 46 (1932); C. Zener, Proc. R. Soc. London Ser. A **137**, 696 (1932).
[6] G. Hirsch, P. J. Bruna, R. J. Buenker, and S. D. Peyerimhoff, Chem. Phys. **45**, 335 (1980).
[7] H. Ågren, A. Flores-Riveros, and H. J. Aa. Jensen, Phys. Rev. A **34**, 4606 (1986).
[8] (a) L. Wolniewicz and K. Dressler, J. Chem. Phys. **88**, 3861 (1988); (b) P. Quadrelli, K. Dressler, and L. Wolniewicz, J. Chem. Phys. **92**, 7461 (1990).
[9] (a) B. H. Lengsfield III, P. Saxe, and D. R. Yarkony, J. Chem. Phys. **81**, 4549 (1984); (b) P. Saxe, B. H. Lengsfield III, and D. Yarkony, Chem. Phys. Lett. **113**, 159 (1985); (c) B. H. Lengsfield III and D. R. Yarkony, J. Chem. Phys. **84**, 348 (1986); (d) P. Saxe and D. R. Yarkony, J. Chem. Phys. **86**, 321 (1987).
[10] J. Olsen and P. Jørgensen, J. Chem. Phys. **82**, 3235 (1985).
[11] T. Helgaker and P. Jørgensen, Adv. Quantum Chem. **19**, 183 (1988).
[12] R. Cimiraglia, in NATO ASI Series Volume, *Time Dependent Quantum Molecular Dynamics: Experiments and Theory*, edited by F. Broeckhove (Plenum, New York, 1992) (submitted).
[13] (a) P. Jørgensen and J. Simons, J. Chem. Phys. **79**, 334 (1983); (b) T. U. Helgaker and J. Almlöf, Int. J. Quantum Chem. **26**, 275 (1984).
[14] SIRIUS, ABACUS, and RESPONS are a suite programs by H. J. Aa. Jensen, P. Jørgensen, T. Helgaker, J. Olsen, H. Ågren, P. Taylor, O. Vahtras, H. Hettema, H. Koch, and K. L. Bak.
[15] J. Augspurger and C. Dykstra, J. Chem. Phys. **88**, 3817 (1988).
[16] W. Kolos, J. Mol. Spectrosc. **62**, 429 (1976).
[17] W. Kolos, J. Mol. Spectrosc. **86**, 420 (1981).
[18] T. E. Sharp, At. Data **2**, 119 (1971).
[19] M. Jaszunski, B. O. Roos, and P. Widmark, J. Chem. Phys. **75**, 306 (1981).
[20] T. H. Dunning, J. Chem. Phys. **90**, 1007 (1989).